X-ray absorption, glancing-angle reflectivity, and theoretical study of the N K- and Ga $M_{2,3}$-edge spectra in GaN

W. R. L. Lambrecht, S. N. Rashkeev,* and B. Segall
Department of Physics, Case Western Reserve University, Cleveland, Ohio 44106-7079

K. Lawniczak-Jablonska,† T. Suski,‡ E. M. Gullikson, J. H. Underwood, and R. C. C. Perera
Lawrence Berkeley National Laboratory, University of California, Berkeley, California 94720

J. C. Rife
Naval Research Laboratory, Washington, D.C. 20375

I. Grzegory and S. Porowski
UNIPRESS, Polish Academy of Sciences, 01-142 Warszawa, Poland

D. K. Wickenden
Applied Physics Laboratory, Johns Hopkins University, Baltimore, Maryland 20723
(Received 1 August 1996; revised manuscript received 16 September 1996)

A comprehensive study of the nitrogen K edge and gallium $M_{2,3}$ edge in gallium nitride is presented. Results of two different experimental techniques, x-ray absorption by total photocurrent measurements and glancing-angle x-ray reflectivity, are presented and compared with each other. First-principles calculations of the (polarization averaged) dielectric response $\epsilon_2(\omega)$ contributions from the relevant core-level to conduction-band transitions and derived spectral functions are used to interpret the data. These calculations are based on the local density approximation (LDA) and use a muffin-tin orbital basis for the band structure and matrix elements. The angular dependence of the x-ray reflectivity is studied and shown to be in good agreement with the theoretical predictions based on Fresnel theory and the magnitude of the calculated x-ray optical response functions. The main peaks in the calculated and measured spectra are compared with those in the relevant partial density of conduction-band states. Assignments are made to particular band transitions and corrections to the LDA are discussed. From the analysis of the N K and Ga $M_{2,3}$ edges the latter are found to be essentially constant up to ~ 10 eV above the conduction-band minimum. The differences in spectral shape found between the various measurements were shown to be a result of polarization dependence. Since the c axis in all the measurements was normal to the sample surface, p-polarized radiation at glancing angles corresponds to $\mathbf{E}\|\mathbf{c}$ while s polarization corresponds to $\mathbf{E}\perp\mathbf{c}$ at all incident angles. Thus, this polarization dependence is a result of the intrinsic anisotropy of the wurtzite structure. Spectra on powders which provide an average of both polarizations as well as separate measurements of reflectivity with s polarization and p polarization were used to arrive at this conclusion. [S0163-1829(97)06404-7]

I. INTRODUCTION

The recent breakthroughs in GaN-based bright light emitting diodes[1] and laser diodes[2] and its promise for high-temperature, high-field, and high-frequency electronic applications[3] have spurred a new interest in the basic properties of this material. While several theoretical studies of the band structure have been published—see Ref. 4 for an overview—relatively few experimental studies of the band structure have been carried out. Photoemission studies[5–7] have been used to probe the occupied valence states directly. UV-reflectivity[8] and spectroscopic ellipsometry[9–11] provide further information on the band structure but contain the information on the conduction bands in a somewhat indirect way requiring theoretical calculations of the dielectric response[8,12,13] for their interpretation. Furthermore, continuum excitonic effects may strongly affect the oscillator strengths of these spectra[12] and complicate a straightforward interpretation in terms of the interband transitions. As was recently pointed out by some of us,[12] the measured UV optical response functions exhibit discrepancies with the one-electron theory which are difficult to reconcile even when self-energy corrections as calculated by Rubio *et al.*[14] and Palummo *et al.*[15] are applied to the local density band-structure results. To further complement these studies, an independent study of the unoccupied conduction-band states is thus desirable.

As is well known the near-edge region of x-ray absorption spectra provides such information since it probes transitions from the core level to the low lying empty conduction band states. In this paper, we present x-ray absorption spectra of GaN in the region of the nitrogen K (N $1s$ to conduction band) and gallium $M_{2,3}$ (Ga $3p_{1/2}$ and Ga $3p_{3/2}$ to conduction band) edges.

In this paper, we present results using two different experimental techniques for probing the x-ray absorption spectra and provide a theoretical analysis of them. In both techniques the samples are exposed to an x-ray beam from a

synchrotron radiation source and the x-ray photon energy is varied over the range of interest. In the first technique the x-rays are oriented at normal incidence to the surface of the sample and the absorption as a function of photon energy is monitored by measuring the total photocurrent. The second technique measures the x-ray reflectivity at glancing angles and deduces the absorption coefficients from that by Kramers-Kronig (KK) analysis. Essentially the latter technique is based on the fact that at glancing angles $\theta \ll 1$, and, when $\epsilon_2 \ll \theta$ and $\epsilon_1 \approx 1$, the Fresnel equations for the reflectivity R reduce to $R \propto |\epsilon - 1|^2$. If $\epsilon_1 - 1 \ll \epsilon_2$, $\sqrt{R}$ gives approximately ϵ_2. The x-ray absorption coefficient $\alpha = 4\pi k/\lambda$ in this limit of small ϵ_2 is also proportional to ϵ_2. Thus, one expects the glancing-angle reflectivity spectra to closely resemble the x-ray absorption spectra for the appropriate choice of angle.

Note, however, that there are three small parameters at play: θ, $\epsilon_1 - 1$, and ϵ_2. For $\theta \to 0$, $R \to 1$ independently of ϵ. One could anticipate that if $\epsilon_2(\omega)$ shows a structure as a function of frequency just above the edge, the conditions on the relative values of these parameters may change appreciably. From this, one can see that a strong angular dependence of the peak intensities is expected. Therefore a careful calculation of $R(\omega, \theta)$ in terms of $\epsilon(\omega)$ and the angle θ is important. In particular, it is important to know the magnitude of the matrix elements with sufficient precision. To this end, we have performed first-principles calculations of the dielectric response function $\epsilon_2(\omega)$ in the x-ray region based on muffin-tin orbital band-structure calculations and from it obtain the desired spectral functions such as $\alpha(\omega)$ and $R(\omega, \theta)$.

Because a significant simplification of the calculation method is obtained by averaging over polarization directions, the present calculations were performed with this restriction. Although this was not evident from the beginning of our study, the combined measurements with the different techniques and the theory eventually showed that polarization effects are present.

To fully appreciate how we arrived at this conclusion, we briefly mention the chronological order of our investigation. The order of presentation of the results in the paper also closely follows this same order, thus providing the reader a sense of why we did the various measurements. The initial x-ray reflectivity measurements were carried out at the National Synchrotron Light Source (NSLS) in Brookhaven and absorption coefficients were obtained from it by KK analysis including the glancing angle conditions and using Fresnel theory. Subsequently, the total photocurrent measurements were done at the Lawrence Berkeley National Laboratory Advanced Lights Source (ALS). Comparison of both of these with the calculated (polarization averaged) results revealed some discrepancies between both experimental results and between theory and experiment which required further study. The x-ray reflectivity measurements were then repeated at ALS as a function of angle and their KK analysis was shown to provide results in excellent agreement with the total photocurrent measurements. The angular dependence was also adequately explained in terms of the calculated spectra. At this moment, one could think that sample differences were the origin of the discrepancies. However, measurents of different types of samples at ALS, including powders, epitaxial films, and bulk single crystals revealed little changes, except for the powders which showed spectra intermediate in shape between those at ALS and those at NSLS and in better agreement with the theory. Finally, it became clear that the difference was due to the fact that the measurements at NSLS had been done under nominal *p* polarization while those at ALS were done under *s*-polarization conditions. By *p* polarization it is meant that the electric field vector of the incident light is in the plane of incidence. Under these conditions, and at glancing incidence on the basal plane of the crystal, the electric field vector is almost parallel to the *c* axis: $\mathbf{E} \| \mathbf{c}$. In *s* polarization, on the other hand, the electric field vector is perpendicular to the plane of incidence and is thus always perpendicular to the *c* axis of the sample, no matter what the incident angle is, as long as the *c* axis is in the plane of incidence. Since the crystal structure is anisotropic, this is expected to lead to differences in intensity. It also explained the very good agreement between the total photocurrent measurements (under normal incidence) and the *s*-polarization reflection measurement at glancing angles. Finally, to fully confirm the polarization dependence, the reflectivity measurements were repeated once more at NSLS in both polarizations. Excellent agreement was obtained with the prior results for *s* polarization at ALS as well as the original *p*-polarized measurements at NSLS. At the same time the measurements were performed over a somewhat wider energy range to refine the KK analysis. It would, of course, be desirable to include the polarization effects directly in the calculations. However, this is postponed until a later study. The experimental evidence of the polarization effect, indeed, speaks for itself. The present calculations even without the explicit inclusion of the polarization allow us to make a detailed analysis of the spectra in terms of the underlying band structure. This was the original goal of the study.

The overall good agreement in peak positions obtained between the independent measurements with the two techniques and on different samples and with the corresponding parameter free theoretical results provides confidence that our measurements represent intrinsic properties of bulk GaN. The theoretical analysis, allows us to assign the peak positions to specific features in the conduction-band partial densities of states. The theory is based on the local density approximation (LDA) to density functional theory[16] which is well known to underestimate the band gap and also to lead to a substantial underestimate of the absolute binding energy of the core levels. We thus do not attempt a comparison between the absolute energies in theory and experiment but merely a comparison between relative positions of peaks. We can thus look for systematic variations in the conduction-band self-energy corrections to the LDA. Both the N *K* edge and Ga $M_{2,3}$ spectra indicate that the shift of the conduction bands is essentially constant up to ~ 10 eV above the conduction-band minimum and does not increase systematically with increasing energy above the minimum. This conclusion agrees with that of the previous UV-reflectivity study,[8] but disagrees with presently available calculations of the self-energy corrections[14] and indicates that further work on these many-body effects is required.

II. THEORY AND COMPUTATIONAL METHODOLOGY

A. Theory of x-ray reflectivity and absorption

The edge spectra that we are interested in correspond essentially to transitions from a core level to the conduction

band. The basic property describing these transitions is their contribution to the imaginary part of the dielectric function given by

$$\epsilon_2(\omega)_{\alpha\alpha}=\frac{e^2}{m^2\omega^2\pi}\sum_n \int_{\mathrm{BZ}} d^3k|\langle \phi_c|-i\hbar\nabla_\alpha|\psi_{nk}\rangle|^2 \times(1-f_n^k)\,\delta(\hbar\omega+E_c-E_n^{\mathbf{k}}), \quad (1)$$

where E_c is the core-level energy, $E_n^{\mathbf{k}}$ is a band energy, and the Fermi factor $(1-f_n^k)$ limits the sum to empty conduction-band states. We expand the conduction-band wave function $|\psi_{nk}\rangle=\Sigma_{RL}C_{RL}^{nk}|\phi_{RL}(E_{nk})\rangle$ in the one-center partial wave components on the sites **R**. Only the site on which the core hole is located will contribute to Eq. (1). We have used the abbreviation $L=(l,m)$. The C_{RL}^{nk} coefficients are the eigenvectors of the linear muffin-tin orbital band-structure problem in the nearly-orthogonal representation.[17] Each $\phi_{RL}(E_{nk},\mathbf{r})$ function is as usual expanded in a Taylor series around an energy E_ν in the center of the bands of interest. Introducing spherical tensor components instead of the Cartesian components α and using the Wigner-Eckart theorem, the matrix elements can be reduced to products of a reduced matrix-element $\langle\phi_{l_c,0}|\nabla_0|\phi_{l,0}\rangle$ and some combination of $3j$ symbols. Furthermore, if we take the average over polarizations, the combination of $3j$ symbols becomes indepedent of m and the whole expression reduces to a sum of the l_c+1 and l_c-1 partial densities of states each multiplied by a radial matrix element. These usual l-dependent but m-independent partial densities of states are significantly easier to calculate than those occuring when polarization is included because only a sum over the irreducible part of the Brillouin zone is required without a need to apply symmetry operations to the matrix elements. Our present computer code utilizes this approach. While the experiments show that the polarization affects the relative intensities of the various peaks, the polarization averaged x-ray optical functions calculated here still are quite useful in interpreting the experimental results.

From $\epsilon_2(\omega)$, we can now obtain all other desired spectral functions. First, $\epsilon_1(\omega)$ is obtained by Kramers-Kronig transformation. The complex index of refraction is obtained from $\mu(\omega)=n(\omega)+ik(\omega)=\sqrt{\epsilon(\omega)}$. The x-ray absorption coefficient is then given by $\alpha(\omega)=4\pi k(\omega)/\lambda$ in terms of the exctinction coefficient $k(\omega)$ and the wavelength λ. This is the spectrum being measured by the total photocurrent method described below.

From the Fresnel equations,[18] the reflectivity $R(\omega,\theta)=|r(\omega,\theta)|^2$ for an incident angle θ is obtained from

$$r(\omega)=\frac{\epsilon\sin\theta-\sqrt{\epsilon-(\cos\theta)^2}}{\epsilon\sin\theta+\sqrt{\epsilon-(\cos\theta)^2}}, \quad (2)$$

for p polarized light (i.e., **E** parallel to the plane of incidence) and by a similar expression but with ϵ replaced by 1 in the first term in nominator and denominator for s-polarized light (**E** perpendicular to the plane of incidence). We have assumed here that the medium from which the light is incident on the sample is vacuum. We chose to use the angle with respect to a vector in the plane rather than measured from the surface normal because we will be interested in small angles θ for which we can approximate $\sin\theta=\theta$ and $(\cos\theta)^2=1-\theta^2$. As $\theta\to0$ clearly $r(\omega)\to-1$ and the reflectivity approaches 1. It is instructive to examine this limit somewhat more closely. In the x-ray ranges of interest the matrix elements are such that $\epsilon_2(\omega)$ is of the order of 10^{-2}. Similarly, the deviations of the real part from 1, i.e., $\tilde{\epsilon}_1=\epsilon_1-1$ are of the order of 10^{-2} and the angle θ is chosen near 5° or θ is of the order of 0.1. Thus $\epsilon-1$ is typically of the same order as θ^2. On the other hand, if $\theta^2\gg|\epsilon-1|$, but still $\theta^2\ll1$, we obtain

$$r(\omega)\approx-\frac{\tilde{\epsilon}_1(\omega)+i\epsilon_2(\omega)}{4\theta^2}. \quad (3)$$

Thus, the reflectivity $R(\omega)\propto|\epsilon-1|^2$ in this case. The same expression is obtained for s-polarized light in this limit. In fact, if $\tilde{\epsilon}_1\ll\epsilon_2$, we see that $R(\omega)\propto\epsilon_2(\omega)^2$. It is thus not surprising that the reflectivity will resemble the x-ray absorption spectrum rather closely. Nevertheless, it is clear that a rather careful analysis including the actual angle of incidence is necessary because if ϵ_2 and $\tilde{\epsilon}_1$ are not known *a priori* one cannot be sure whether the condition $\theta^2\gg|\epsilon-1|$ is satisfied or not. Of course, for $\theta\to0$ $r(\omega)$ does not diverge but approaches -1 because for $\theta^2<|\epsilon-1|$, the above approximation is no longer valid.

B. Band-structure computational method

The band-structure and matrix-element calculations were performed using the linearized muffin-tin orbital method[17] in the same manner as in previous work on the UV reflectivity.[8] The atomic sphere approximation was employed with two different size empty spheres introduced to fill the characteristic open spaces in the wurtzite lattice. The experimental lattice constants were adopted. Spin-orbit coupling is included for the core level while the valence- and conduction-band states were calculated scalar relativistically.

The crystal potential is obtained self-consistently using the LDA (Ref. 19) to density functional theory.[16] It is important to keep in mind that this is a theory for ground state properties and that its Kohn-Sham eigenvalues do not strictly speaking represent one-electron excitation energies. The latter differ from the former by a self-energy correction. In the present case, there are two important corrections to consider. First, the conduction bands should be shifted up by an approximately 1 eV gap correction.[8,14,15] While a previous study of UV reflectivity[8] suggested a more or less constant correction of the conduction bands up to about 10 eV above the conduction-band minimum, the calculations by Rubio *et al.*[14] using Hedin's[20] so-called ''GW'' approximation—in which G stands for the one electron Green's function and W for the screened Coulomb interaction—indicate a trend of increasing shifts of the conduction-band states with increasing energy above the minimum.

Secondly, the core levels are shifted down from the LDA value by a shift of several eV. The origin of the core-level shifts is explained in more detail in Ref. 7 to consist of two main contributions: a self-interaction correction and a final-state screening correction. Calculations of these within the excited atom model as in Ref. 7 still have an estimated error of a few eV for these deep core levels. Without embarking

on a separate calculation treating the core hole as a point defect, which is beyond the scope of the present work, this prevents us from calculating the absolute position of the edges with adequate precision. We can thus presently only compare relative positions of peaks after the first peaks are adjusted empirically. On the other hand, we can also compare with x-ray photoelectron spectroscopy (XPS) measurements of the core-level binding energies.[21]

III. EXPERIMENT

A. X-ray glancing-angle reflectivity and its Kramers-Kronig analysis

Initial reflectance measurements were performed on the Naval Research Laboratory beamline X24C at the National Synchrotron Light Source.[24] The monochromator delivered radiation with a resolving power of about 1200 (0.3 to 0.4 eV at 400 eV) with two 2400 l/mm gratings in the series. Second order and scattered light from the monochromator were suppressed by a 1600 Å thick Ti filter for the N K data and a 3300 Å thick B filter for the Ga M_{23} data. The Ti L_3 edge provided a check of the energy calibration. At the N K edge, radiation from the exit slit had a relatively flat spectrum but with 10% dips at 399 and 406 eV due to nitrogen compounds on the beamline grazing optics. The reflectance measurements were made with a ultrahigh vacuum reflectometer and had an angular accuracy of $\pm 0.1°$.[25] The reflected radiation as well as the incident was measured with the same $Ga_xAs_{1-x}P$ photodiode detector and the ratio taken to determine the reflectance. The radiation from the exit slit was better than 90% linearly polarized at 400 eV and better than 95% at 100 eV in the orbital plane of the synchrotron. Reflectance was first measured in nominal p polarization, as defined in the introduction. Subsequently, prompted by the differences observed between these initial measurements and the ones obtained at ALS (described in the next section), the measurements at NSLS were repeated in both s and p polarization, clearly evidencing the polarization dependence.

A KK analysis of the data was done in the manner of Veal and Paulikas[26] with Lorentz oscillators to fit extrapolations to low and high energies. This was modified to accommodate glancing reflectance measurements in s polarization by Roessler.[27] Since the difference in the Fresnel equations between s and p reflectance is small for our case [see the discussion after Eq. (3) in Sec. II], good results are also obtained for p polarization. Of course, for the p-polarized measurements, the results still represent p-polarized optical constants. Using optical constants from 4 to 30 eV derived by KK analysis from near-normal reflectance of a previous paper,[8] the reflectance was generated at 5° grazing from 0.1 eV to 30 eV. Reflectance measurements from 95 to 135 eV were also used. For the KK analysis, the glancing reflectance at 5° was interpolated from 30 to 95 eV and 135 to 395 eV and extrapolated above 450 eV. Additional measurements down to 300 eV were used to refine these interpolations. Interpolations and the extrapolation were adjusted to match the reflectance magnitudes and slopes at the boundaries with the data.

B. X-ray absorption and variable angle reflectivity

X-ray absorption and x-ray reflectivity spectra for different incident angles have been collected at the bending magnet 6.3.2. beamline of the ALS. The high photon flux (10^{13}/s/0.1% bandwidth in the N K-edge region) and the high-energy resolution at this beamline allowed us to resolve a fine structure of the x-ray absorption spectra at the K edges of nitrogen and $M_{2,3}$ edge of Ga and to detect a reflected signal even for angles significantly differing from the optimal glancing angle. The detailed description of the originally designed plane grating Hettrick-Underwood type varied line space monochromator and mirrors set at this station can be found elsewhere.[22] The investigated samples were stuck into a conducting indium foil which was isolated from the sample holder in the ultra high vacuum reflectometer. The reflectometer has a capability of positioning the sample to 10 μm and setting its angular position to 0.002°. For measurements in the absorption mode, the direct photocurrent from the sample, positioned perpendicularly to the x-ray beam, was measured as a function of the incoming radiation energy. The intensity of the incoming radiation was monitored by the photocurrent (I_0) generated at the focusing mirror. No structure of this photocurrent due to beamline optics was detected in the energy range under interest. Therefore, no filters were used. The storage ring was operated at the energy of 1.5 GeV with current between 400 and 250 mA. The polarization vector of the radiation was parallel to the plane of the ring and along the axis (in the c plane) around which the sample was rotated. This implies that the polarization was transverse electric (also called s polarization), i.e., with the electric field normal to the plane of the incident and reflected light beams. This implies $\mathbf{E} \perp \mathbf{c}$ for all measurements as already indicated in the introduction.

The resolving power E/dE of the 1200 l/mm grating employed (with exit slit 50 μm) was close to 2500 at the K edge of N. This resolution was high enough to distinguish the fine structure in the spectra. An increase of resolving power up to 7000 (exit slit 20 μm) did not result in resolving any additional structure in the measured spectra but significantly decreased the signal intensity. The $M_{2,3}$ edge of Ga was measured using a 300 l/mm grating with 50 μm slit, which results in a resolving power of 3000.

In the reflection mode, the resolution was kept the same but the reflected radiation was detected by $Ga_xAs_{1-x}P$ photodiode positioned at the angle 2θ (where θ is the angle between sample surface and incident beam). The position of sample was carefully adjusted using x, y, z, and θ manipulators to provide the best intensity. The error in the θ determination, resulting from the zero angle adjustment due to positioning of the samples in the sample holder, was estimated to be not larger than 0.5°. As will be discussed in detail below, the absolute intensity of the reflectivity drops rapidly when the angle is varied slightly from the optimal glancing incidence angle which was found to be 5.3°. The high flux of the beamline and a high detector sensitivity enabled us to register clear structure of the reflected beam at the angles up to 9°. This fact was important for the evaluation of the angular dependence of the real and imaginary part of the GaN dielectric function.

The $M_{2,3}$ edge of Ga was not very pronounced and positioned on a structureless background which decreased strongly with decreasing of the incident beam energy. That results from a significant decrease of the grating efficiency in this energy range. Therefore, a normalization procedure (dividing by I_0) and linear background subtraction was applied.

C. Samples

The samples used in the NSLS study were grown at the Applied Physics Laboratory as epitaxial films on sapphire by metalorganic chemical vapor deposition. The samples are the same as those used in the previous UV reflectivity study[8] and more details on the sample preparation can be found in that paper.

Three kinds of GaN samples were used in x-ray absorption experiments. GaN powder (with particle size smaller than 20 μm available commercially), epitaxial film of about 1 μm thick grown by molecular beam epitaxy on sapphire substrate, and bulk single crystal of GaN, grown by a high pressure, high-temperature method.[23] The latter sample had the form of a platelet perpendicular to the hexagonal c axis. The epitaxial films had the same orientation. To verify the low sensitivity of this method to the sample surface roughness and contaminations, these three kinds of GaN samples were employed. In variable angle reflectivity measurements only the epitaxial film was used.

IV. RESULTS AND DISCUSSION

A. Nitrogen *K* edge

1. Reflectivity and Kramers-Kronig analysis

The top panel in Fig. 1 shows the glancing angle x-ray reflectivity of GaN in the N K-edge region. This spectrum was measured with $\theta = 5.1 \pm 0.1°$ with p-polarized light. The second panel shows the absorption coefficient $\alpha(\omega)$ extracted from it by Kramers-Kronig analysis along with the first-principles calculation of the same spectrum.

We note that there is a substantial difference in peak intensities between the reflectivity spectrum and the absorption spectrum indicating that the condition $\theta^2 \gg |\epsilon - 1|$ is not satisfied for this angle. In particular, this is seen to lead to a shift of intensity from the first two peaks which appear as only small shoulders below the third peak in the reflectivity spectrum.

The experimental and theoretical absorption spectra are in satisfactory agreement although there are clearly some shifts in peak positions as well as differences in intensity. The corresponding peaks in the experimental and theoretical absorption spectra are labeled by uppercase and lowercase letters respectively, to clarify our peak by peak assignment and to simplify later discussion.

As far as absolute intensity is concerned, the theory and experiment differ by a factor of about two. This discrepancy should not cause great concern in view of the various factors which may influence absolute intensities. On the experimental side, surface roughness induced diffuse scattering may lead to losses in the reflectance. The very rapid variation of the reflectivity with angle (see Sec. IV A 2) also causes considerable uncertainties in the absolute magnitude of the extracted absorption curve. There are further uncertainties in the extrapolations in the KK analysis as mentioned above and possibly incompletely suppressed spectral impurities. On the theoretical side, a slightly incomplete convergence of angular momentum expansions of the wave functions may influence the magnitude of the matrix elements considerably and there are possibly many-body effects on the oscillator strengths not included in the present theory. In view of these various factors agreement within a factor of 2 is actually gratifying.

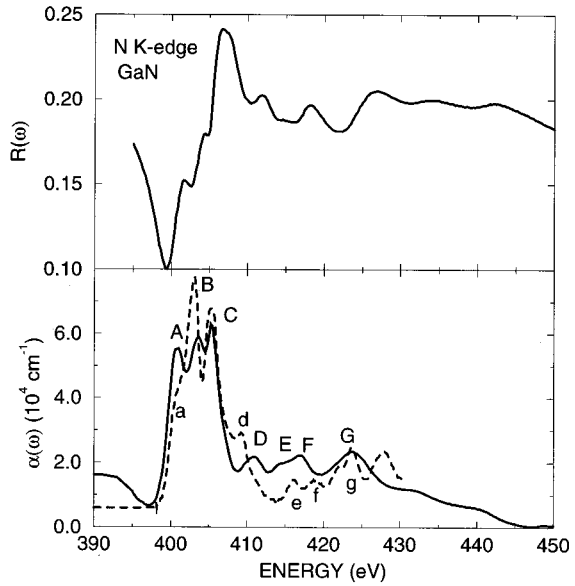

FIG. 1. Nitrogen K edge of GaN as measured by glancing-angle x-ray reflectivity $R(\omega)$ in the top and the x-ray absorption $\alpha(\omega)$ extracted from it by Kramers-Kronig analysis in the bottom panel: Expt. (solid line) compared to calculated spectrum (dashed line). A constant background of 8.9 was subtracted from the experimental absorption spectrum and a constant upward shift of 23.1 eV was applied to the theoretical spectrum.

The shift of our calculated spectrum required to align the first peak is 23.1 eV. From this, we deduce a binding energy of the N $1s$ core level with respect to the conduction-band minimum of 398.6 eV. Subtracting the room temperature gap of 3.4 eV we obtain a binding energy of 395.2 eV with respect to the valence-band maximum in excellent agreement with the XPS results of Martin *et al.*[21] which also gave 395.2 eV. We estimate the error bar on both measurements to be a few 0.1 eV because a peak alignment procedure is involved in each.

Figure 2 shows a direct comparison of the reflectivity to theory. A linear background was subtracted from the experiment to facilitate the comparison. Good agreement is obtained between the theoretical and experimental peak positions. The theoretical curve was actually calculated at a slightly smaller angle than the experimental conditions in order to adjust the absolute magnitude for easy comparison. As discussed above it makes no sense to attempt to reproduce the absolute magnitudes exactly because of the various uncertainties involved.

2. Angular dependence of x-ray reflectivity

As mentioned in the theory section, the x-ray reflectivity at glancing angles is expected to be strongly angular depen-

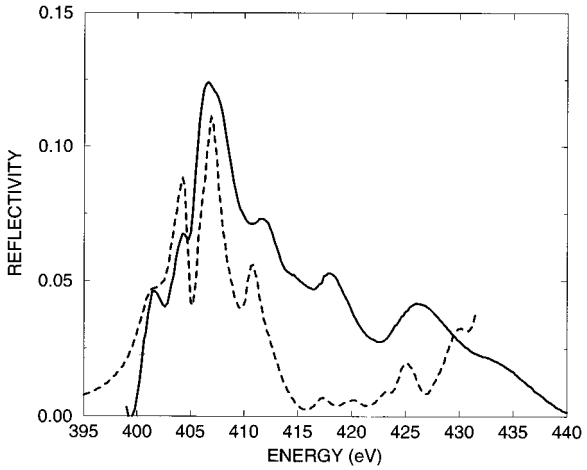

FIG. 2. Nitrogen K-edge reflectivity: comparison to theory. Experiment at 5° glancing incidence using p-polarized light (from Fig. 1) is shown by a solid line after linear background subtraction in range 400–440 eV.

dent. The reflection spectra as function of angle (measured at ALS) are shown in Fig. 3. For easy comparison the collected spectra are normalized. Intensities of reflected radiation measured at a given angle are multiplied by the factor indicated

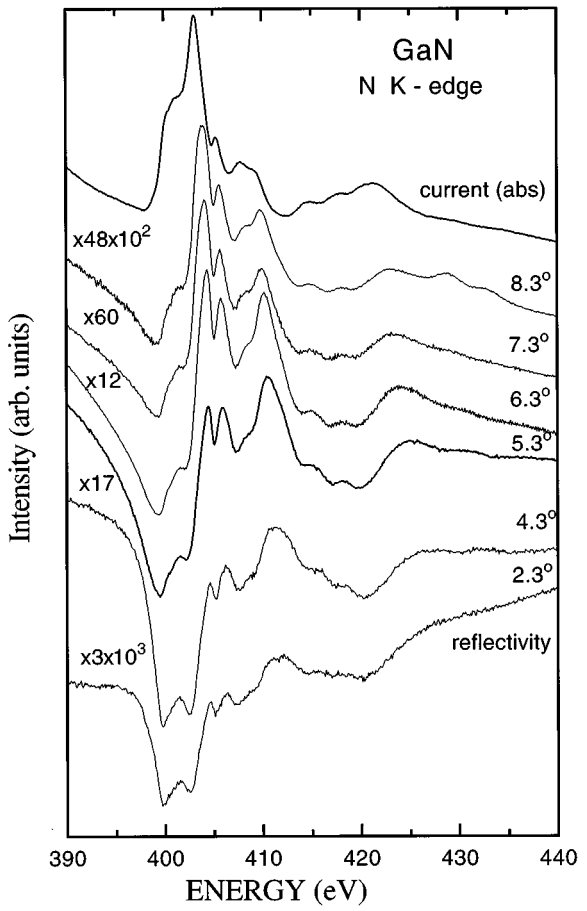

FIG. 3. Normalized reflectivity spectra of the Nitrogen K edge as function of angle. Normalization factors are indicated for each curve, except for the 5.3° case where it is one. The spectra are arbitrarily shifted vertically for convenience. The topmost curve gives the photoyield measurement of the absorption spectrum for comparison.

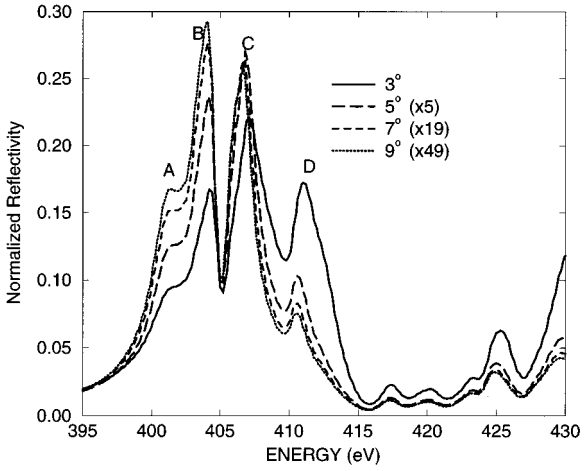

FIG. 4. Calculated dependence of the nitrogen K-edge reflectivity spectrum on incident angle. The spectra were multiplied by the factor indicated to make them coincide at 395 eV.

on the low-energy part of each spectrum. The measured intensity of the reflected beam varies drastically with the value of θ. The glancing angle corresponding to the maximum intensity is equal to 5.3°. It is worthwhile to notice that a decrease of θ by 1° leads to a reduction of the signal intensity by a factor of 17 with a simultaneous increase of the background signal whereas an increase of θ by 1° leads to a reduction of all signal intensity by a factor 12.

The rapid decrease of intensity with increasing angles is easily understood on the basis of the Fresnel equations discussed in Sec. II. In fact, in the limit where Eq. (3) is valid, the reflectivity $R(\omega)$ would vary inversely with θ^4. The rapid decrease of signal amplitude for angles below 5.3° is an indication of the rapid decrease of the penetration depth into the bulk. Therefore, for small angles, the oxygen and carbon contamination layers of the surface may overwhelm the GaN signal and only an increase of the background signal can be seen. The simultaneously measured photocurrent for different angles also shows a drastical change of the N K-edge shape and intensity.

Besides the obvious variation of the intensity there are also more subtle changes of the spectral shape with angle. One can see that at the larger angles, the spectrum resembles the photocurrent measurements more closely as expected from the theoretical considerations. At the lower angles the characteristic negative dip before the onset of the spectrum can be seen and the intensity is shifted towards higher energies.

The calculated spectra at a series of angles are shown in Fig. 4. Here we have chosen to scale the spectra by multiplying with a constant factor so as to make them coincide just below the edge at 395 eV. First of all, we see again that the required multiplication factors vary roughly as expected. A θ^4 dependence would require a multiplication by 7, 30, and 81 for the 5°, 7°, and 9° spectra relative to the 3° spectrum. Second, we see that the shoulder A and peaks B and C increase with increasing angle while the peak D decreases. This is consistent with the data. It shows that the Fresnel theory accounts well for the angular dependence. The reflectivities shown here, show differences from the one in Fig. 1, even when considering the same angle, which we will later show to be a result of the different polarization.

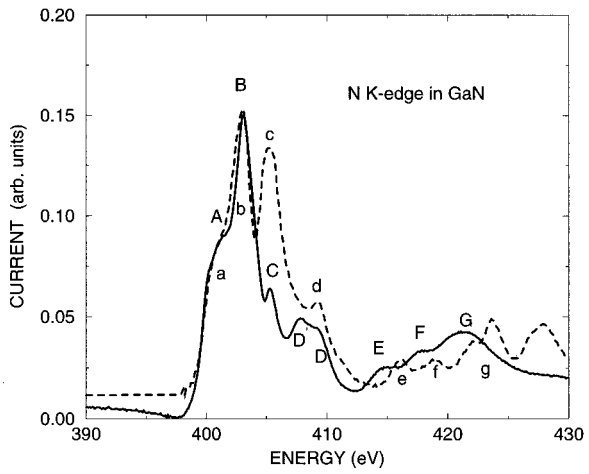

FIG. 5. Nitrogen *K*-edge x-ray absorption spectrum of GaN as measured by total photocurrent (solid line) compared to theory (dashed line).

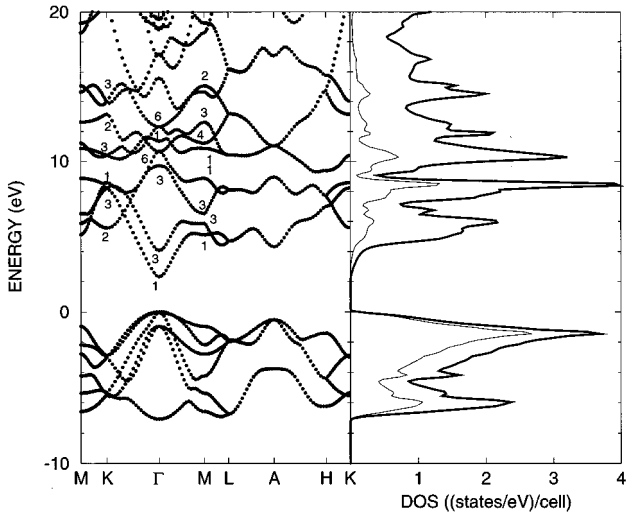

FIG. 6. Band structure and density of states (DOS) in wurtzite GaN. Thin line indicates N $2p$ partial DOS. Conduction-band states at Γ, M, and K are symmetry labeled.

3. Absorption by total photoyield

Figure 5 shows the N *K*-edge x-ray absorption spectrum of GaN as measured by total photocurrent compared to the calculated spectrum. The spectrum shown is I/I_0 after fitting I_0 to a straight line in the energy range of interest. The same shift (23.1 eV) of the theoretical curve used in Fig. 1 was applied here. While the relative peak intensities are somewhat different and also different from the spectrum extracted from x-ray reflectivity in Fig. 1, the peak positions are in good agreement at least up to 10 eV above the edge. In the next subsections, we first discuss the peak positions obtained from the present and previous measurements and subsequently the differences in peak intensities.

4. Band-structure assignment

As mentioned already in the theory section, one expects the N *K*-edge spectra to be essentially proportional to the N $2p$ partial density of states (PDOS). By comparison to the band structure, we can to some extent associate the peaks in partial density of states to van Hove singularities at specific points in the Brillouin zone. Figure 6 shows the band structure of GaN along with the total and N $2p$ partial density of states. The valence-band maximum is chosen as energy reference. For the present purposes only the conduction band is of importance.

Table I compares the experimental and theoretical peak positions from the N *K*-edge spectrum and provides this band-structure assignment. Several **k** points or rather the ''flat band'' regions near to them contribute to each peak. For the first 3 peaks (A–C), no significant differences between theory and experiment are found, indicating that the self-energy correction is approximately constant in that energy range.

This is consistent with a previous UV-reflectivity study.[8] In contrast, the *GW* calculations of Rubio *et al.*[14] indicate a gradually increasing self-energy shift with increasing energy in the conduction band. They obtain about a 1 eV higher shift at about 5 eV above the conduction-band minimum than at the minimum itself. The present comparison between LDA theory and experiment does not seem to give any evidence of such a systematic increase in self-energy correction.

Peak d in the present experiment appears to be split in two peaks, D and D'. The k-point assignment in Table I shows that this peak is expected to arise at least partially from transitions near the second Γ_6 conduction band. The latter is subject to a spin-orbit splitting not included in the present band-structure calculation. A separate calculation of the bands including spin-orbit coupling indicates that this splitting is about 2 eV, consistent with the 1.6 eV splitting of the D–D' peak splitting. In the KK deduced absorption spectrum shown in Fig. 1, this splitting is not resolved and the peak appears to occur at slightly larger energy. In the next section we will show that this is a polarization effect. The Γ_6 state corresponds to p-like states in the basal plane of the crystal and thus transitions to it from the N $1s$ core hole only occur for $\mathbf{E}\perp\mathbf{c}$. The D peak in the other polarization must thus come from other regions of the Brillouin zone.

Above 410 eV, one may note a systematic overestimate of the peak positions by about 1.5 eV by the theory. This is also the case for the KK deduced results except for peak G, which is in good agreement with theory and hence shifted upwards from the photoyield results. The G peak is actually split into two peaks in the theory and a shift of intensity in the data from the lower to the higher-energy part might explain an apparent shift towards higher energy compared to the photoyield data. As will be discussed in the next section, such intensity differences occur also in other parts of the spectrum and may be attributed to a polarization dependence not included in our present theory and different in the two experimental measurements.

For these higher lying bands, we note that the present ''single panel'' linearized muffin-tin orbital method becomes somewhat less reliable because the latter is optimized for states close to the gap. We thus refrain from drawing conclusions about corrections beyond LDA on these bands and conclude that agreement of the overall structure of the spectra to within an eV or so is quite satisfactory.

5. Discussion of intensity differences

We now discuss peak intensity differences between the various spectra. The first peak B and its low-energy shoulder

TABLE I. Experimental and theoretical N *K* peak positions and their band-structure assignment.

Label	KK (*p* polarization)	Photocurrent and KK (*s* polarization)	Theory	*k* points
A	400.7	401.0	400.7	M_1, M_3
B	403.6	403.0	403.0	K_3, K_1, $L_{1,3}$
C	405.2	405.2	405.2	K_3, Γ_6, M_1
D	410.9	409.2	409.2	M_3, Γ_6
E	414.4	414.5	416.9	M_2
F	417.0	417.6	418.8	
G	423.4	421.4	423.3	

A in the total photoyield are in particularly good agreement with theory both in shape and position. Peak *c* is strongly suppressed in the experiment in contrast to the KK extracted spectrum where it is comparable in intensity to the *B* peak. We now show that these differences are evidence of a polarization dependence. As already mentioned in the introduction, the absorption spectra correspond essentially to $\mathbf{E}\perp\mathbf{c}$ because the light is normally incident while the spectrum deduced from x-ray reflectivity by KK corresponds essentially to $\mathbf{E}\|\mathbf{c}$ because the light is *p* polarized and incident close to glancing incidence. The theory as mentioned earlier corresponds to an average of both polarizations.

To check this further as well as the influence of roughness and crystalline perfection, a series of N *K*-edge absorption spectra were taken on three different samples: a powder, an epitaxial film, and a bulk single crystal. These are shown in Fig. 7. No significant differences between the spectra of the epitaxial film and the single crystal were detected indicating the high quality of the epitaxial film. On the other hand, the powder spectrum shows more pronounced *A* and *C* peaks. We interpret these changes in terms of the dependence of the spectra on polarization. The randomly oriented crystallites in the powder should lead to a mixture of $\mathbf{E}\|\mathbf{c}$ and $\mathbf{E}\perp\mathbf{c}$ components in the spectrum. As shown by the comparison of the KK derived absorption spectrum for $\mathbf{E}\|\mathbf{c}$ with the photoyield absorption spectrum for $\mathbf{E}\perp\mathbf{c}$, this should indeed enhance the *A* and *C* peaks compared to the *B* peak. The powder spectrum being an average of both should then most closely resemble our present calculation, which it does.

As is discussed in detail in Sec. IV A 2, x-ray reflectivity was also measured at ALS on the same samples and immediately after the absorption data were taken. A Kramers-Kronig analysis of these reflectivity data (which are shown in Fig. 3) performed in a similar manner as that for the NSLS data provides the absorption spectra shown in Fig. 8. These spectra are in excellent agreement with the total photoyield measurement. Because of the *s* polarization, one expects these spectra to correspond to $\mathbf{E}\perp\mathbf{c}$ independent of the incidence angle, unlike the data obtained at NSLS which correspond to $\mathbf{E}\|\mathbf{c}$. The spectra confirm that there is little dependence on the angle and again are consistent with our interpretation of the polarization dependence as the prime source of difference between the ALS and NSLS data discussed sofar.

Finally, to fully confirm the polarization dependence, the glancing-angle reflectivity spectra were remeasured at NSLS on the same sample in both polarizations. The results for the reflectivity and the KK derived absorption coefficients are shown in Fig. 9. They clearly show excellent agreement with all the previous results and fully confirm the above interpretation. This rules out any alternative explanations such as sample dependence. In fact, the sample independence indicates that our results truely correspond to intrinsic properties of bulk GaN. It also confirms that the apparent shifts of the

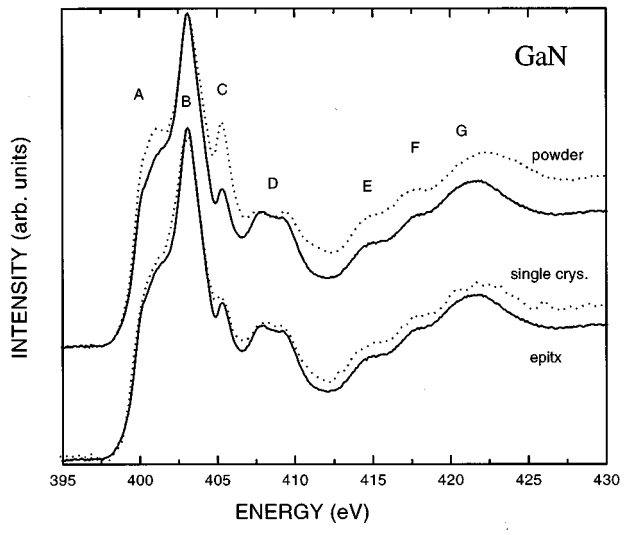

FIG. 7. Measured absorption spectrum for an epitaxial film (solid lines, reproduced and shifted for convenience) compared to that for a single crystal and for a powder sample (dashed lines).

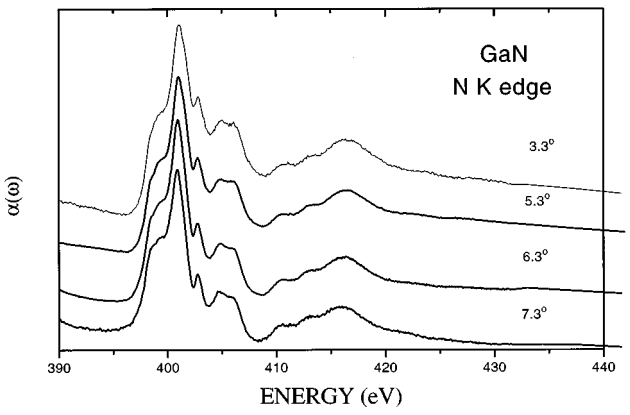

FIG. 8. Absorption spectra obtained by Kramer-Kronig analysis from reflectivity at various incident angles using *s*-polarized light.

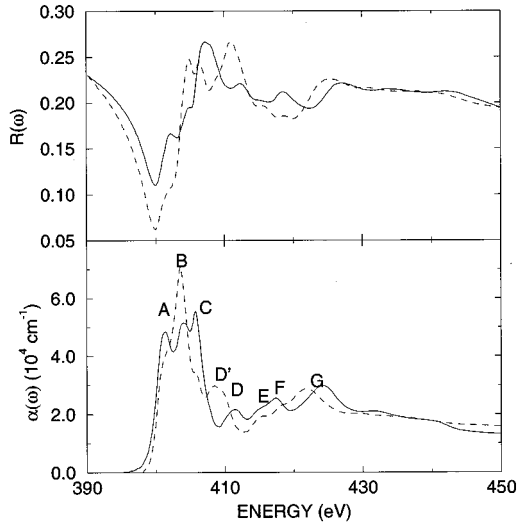

FIG. 9. Reflectivity (upper panel) and absorption spectra (lower panel) obtained by Kramers-Kronig analysis under both *s*- (dashed line) and *p*-polarized (solid line) light on the same sample.

D, *D′*, and *G* peaks which were noted above are purely due to the polarization effect.

Still, a weighted average of the *s*- and *p*-polarized spectra does not fully agree with the theory, indicating that other aspects not fully included in the present theoretical treatment affect the intensities. It is well known that many-body effects exist on x-ray absorption spectra and may be responsible for these remaining deviations. This includes among others, the effect of the localized core hole in the final state on the local density of states which may differ from that of the unperturbed crystal. While this can, in principle, be included by treating the core hole as a localized defect, such calculations are far more time consuming than the present ones and outside the scope of the present paper.

B. Ga $M_{2,3}$ edge and M_1 edges

Figure 10 shows the glancing-angle x-ray reflectivity for the Ga $M_{2,3}$ edge. This spectrum is rather broad because of the overlap of the spin-orbit split $3p_{1/2}$ and $3p_{3/2}$ contributions. The agreement with the calculated reflectivity calculated under the glancing-angle conditions is satisfactory. Again, absolute values were adjusted arbitrarily.

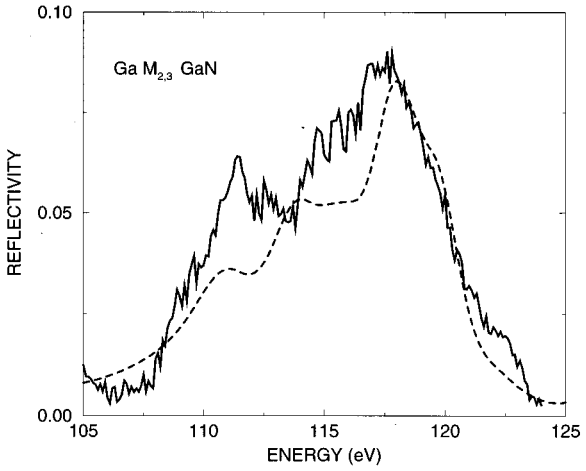

FIG. 10. Gallium $M_{2,3}$ edge of GaN as measured by glancing angle x-ray reflectivity (solid line) compared to theory (dashed line).

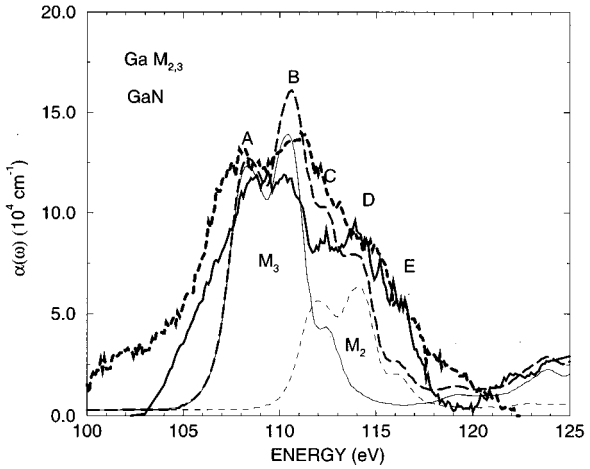

FIG. 11. Gallium $M_{2,3}$ edge of x-ray absorption spectrum of GaN as measured by total photocurrent (thick short-dashed line), and from KK analysis of reflectivity (thick solid line) compared to theory (long dashed line). Separate calculated contributions of $3p_{1/2}$ and $3p_{3/2}$ are indicated by thin dashed and thin solid lines, respectively. A shift of 10.7 eV was applied to the theory.

Figure 11 shows the Ga $M_{2,3}$ x-ray absorption spectrum both as measured directly from total photoyield and by KK analysis of the reflectivity data of the previous section compared to the calculated results. The separate M_2, M_3 contributions are also indicated. Good agreement is obtained. The shift applied to the theoretical spectrum in this case is 10.7 eV. This results in a binding energy of the Ga $3p_{3/2}$ state with respect to the valence-band maximum of 101.9 eV in good agreeement with the XPS results which gave 102.6 eV. Our calculated spin-orbit splitting between Ga $3p_{1/2}$ and $3p_{3/2}$ of 3.65 eV is also in good agreement with the XPS result of 3.7 eV.[21]

We note that the *A* and *B* peaks correspond to the Ga M_3 spectrum while the *C* peak is an overlap of the first peak of the M_2 spectrum and the third (much weaker) peak of the M_3 spectrum. Peaks *D* and *E* correspond to the M_2 spectrum.

From the Ga $M_{2,3}$ spectrum we deduce the same equal ~ 2 eV spacing between the first three peaks in the conduction band as was deduced from the N *K*-spectrum in Sec. IV A. The peak positions are about 108, 110, and 112 eV for *A*, *B*, *C* corresponding to M_3 and 112, 114, and 116 eV for *C*, *D*, *E* in the M_2 spectrum. The same conclusion about the constant shift nature of the conduction-band energy correction beyond the LDA is thus deduced from the Ga $M_{2,3}$ as it was from the N *K* spectra.

Figure 12 shows the calculated Ga $M_{2,3}$ spectrum over a wider energy range (including transitions to about 70 bands) extending into the region where the M_1 edge is expected. It is shown that transitions from Ga $3p$ to high lying conduction states overlap with the transitions from Ga $3s$ to the bottom of the conduction band. The latter are much weaker because of the smaller matrix elements and hence are difficult to observe. This is seen by separately plotting a spec-

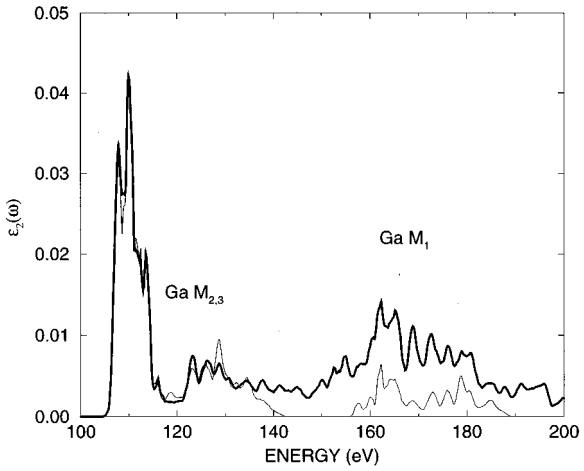

FIG. 12. Calculated $\epsilon_2(\omega)$ function in an energy range above the Ga $M_{2,3}$ edge which includes the Ga M_1 edge region, including transitions to about 70 bands. Separate $M_{2,3}$ and M_1 spectra corresponding to transitions to lower 30 conduction bands only are indicated by a thin line.

trum in which only transitions to the lower 30 conduction bands are included as shown by the thin line in Fig. 12. We caution that the higher conduction bands may not be very accurately reproduced by our linearized muffin-tin orbital method which is designed to calculate bands only within about 1 Ry from the Fermi energy. Also, a slightly different self-energy shift is expected for the $3s$ and the $3p$ core holes.

Experimentally, the M_1 edge was detected in our ALS measurements at the expected position of 162 eV as a steplike feature. Since no detailed structure could be resolved, the spectrum is not shown here.

V. CONCLUSIONS

We have presented a systematic study of the N K- and Ga $M_{2,3}$-edge spectra in GaN and detected the presence of the Ga M_1 edge. Aside from some small discrepancies, consistent results were obtained for the peak positions from two different experimental techniques employed to probe these spectra: glancing incidence angle x-ray reflectivity combined with Kramers-Kronig analysis and total photocurrent measurements of the x-ray absorption. Both sets of experimental data agree well with calculated spectra, especially for the transitions to the lower conduction-band states up to about 10 eV above the conduction-band edge. Even up to 20 eV above the conduction band minima the agreement in spectral shape is rather good with maximum discrepancies between theory and experimental peak positions of about 1 eV. The absolute energies of the edges were also shown to be consistent with XPS measurements of the core-level binding energies with respect to the valence-band maximum.

The good agreement in peak positions and the assignment of the peaks to the band-structure features allows us to conclude that the self-energy correction beyond the LDA band-structure consists essentially of a constant shift for the conduction bands up to about 10 eV above the conduction-band minimum. No systematic increase in the correction with increasing conduction-band energy could be identified. This is in disagreement with presently available *GW* calculations which predict a trend of increasing corrections for higher-energy conduction-band states. This indicates a need for further work in this area.

Some differences in peak intensities were observed between theory and between the two original sets of experiment. The different polarizations involved in the two experimental setups used was clearly shown to be the origin of these differences by several means but most definitively by remeasuring the same sample under both polarizations. The present calculations did not include polarization because averaging over polarization directions constitutes a significant computational simplification. We plan to include it in future work now that the experimental evidence for this effect has been clearly established to be important. Further differences between theory and experiment may arise from a core-hole final state and other many-body effects not included in the present theoretical treatment. Future work to address these questions is planned.

ACKNOWLEDGMENTS

The work at CWRU was funded by the National Science Foundation under Grants Nos. DMR 93-22387 and DMR 95-29376. The reflectance measurements were performed at the National Synchrotron Light Source which is sponsored by the U.S. Department of Energy and at the Advanced Light Source which is sponsored by U.S. Department of Energy under Contract No. DE-AC03-76SF00098. K.L-J. and T.S. kindly acknowledge the financial support of the Fulbright Foundation.

*Permanent address: P. N. Lebedev Physical Institute, Russian Academy of Sciences, 117924 Moscow, Russia.

†Permanent address: Institute of Physics, Polish Academy of Sciences, 02-668 Warszawa, Poland.

‡Permanent address: UNIPRESS, Polish Academy of Sciences, 01-142 Warszawa, Poland.

[1] S. Nakamura, M. Senoh, N. Iwasa, and S. Nagahama, Jpn. J. Appl. Phys. **34**, L797 (1995); S. Nakamura, M. Senoh, N. Iwasa, Nagahama, T. Yamada, and T. Mukai, *ibid.* **34**, L1332 (1995).

[2] S. Nakamura, M. Senoh, S. Nagahama, N. Iwasa, T. Yamada, T. Matsushita, H. Kiyoku, and W. Sugimoto, Jpn. J. Appl. Phys. **35**, L74 (1996).

[3] See, e.g., *Gallium Nitride and Related Materials*, edited by R. D. Dupuis, J. A. Edmond, F. Ponce, and S. Nakamura, MRS Symposia Proceedings No. 395 (Materials, Research Society, 1996).

[4] W. R. L. Lambrecht and B. Segall, in *Properties of Group III Nitrides*, edited by J. H. Edgar, Electronic Materials Information Service (EMIS) Datareviews Series (Institution of Electrical Engineers, London, 1994), Chap. 4.

[5] J. Hedman and N. Mårtenson, Phys. Scr. **22**, 176 (1988).

[6] R. W. Hunt, L. Vanzetti, T. Castro, K. M. Chen, L. Sorba, P. I. Cohen, W. Gladfelter, J. Van Hove, A. Kahn, and A. Franciosi, Physica B **185**, 415 (1993).

[7] W. R. L. Lambrecht, B. Segall, S. Strite, G. Martin, A. Agarwal, H. Morkoc, and A. Rockett, Phys. Rev. B **50**, 14 155 (1994).

[8] W. R. L. Lambrecht, B. Segall, J. Rife, W. R. Hunter, and D. K.

Wickenden, Phys. Rev. B **51**, 13 516 (1995).
[9] J. Petalas, S. Logothetidis, S. Boultadakis, M. Alouani, and J. M. Wills, Phys. Rev. B **52**, 8082 (1995).
[10] S. Logothetidis, J. Petalas, M. Cardona, and T. D. Moustakas, Phys. Rev. B **50**, 18 017 (1994).
[11] C. Janowitz, M. Cardona, R. L. Johnson, T. Cheng, T. Foxon, O. Günther, and G. Jungk, BESSY Annual Report, 1994 (unpublished), p. 230.
[12] W. R. L. Lambrecht, K. Kim, S. N. Rashkeev, and B. Segall, in *Gallium Nitride and Related Materials* (Ref. 3), p. 455.
[13] N. E. Christensen and I. Gorczyca, Phys. Rev. B **50**, 4397 (1994).
[14] A. Rubio, J. L. Corkill, M. L. Cohen, E. L. Shirley, and S. G. Louie, Phys. Rev. B **48**, 11 810 (1993).
[15] M. Palummo, L. Reining, R. W. Godby, C. M. Bertoni, and N. Börnsen, Europhys. Lett. **26**, 607 (1994); and in *Proceedings of the 21st International Conference on the Physics of Semiconductors*, edited by Ping Jiang and Hou-Zhi Zheng (World Scientific Press, Singapore, 1993), p. 89.
[16] P. Hohenberg and W. Kohn, Phys. Rev. **136**, B864 (1964); W. Kohn and L. J. Sham, *ibid.* **140**, A1133 (1965).
[17] O. K. Andersen, O. Jepsen, and M. Šob, in *Electronic Band Structure and its Applications*, edited by M. Yussouff (Springer, Heidelberg, 1987), p. 1.
[18] J. D. Jackson, *Classical Electrodynamics*, Second ed. (Wiley, New York 1975), Chap. 7.
[19] L. Hedin and B. I. Lundqvist, J. Phys. C **4**, 2064 (1971).
[20] L. Hedin and S. Lundqvist, in *Solid State Physics: Advances in Research and Applications*, edited by F. Seitz, D. Turnbull, and H. Ehrenreich (Academic, New York, 1969), Vol. 23, p. 1.
[21] G. Martin, S. Strite, A. Botchkarev, A. Agarwal, A. Rockett, H. Morkoç, W. R. L. Lambrecht, and B. Segall, Appl. Phys. Lett. **65**, 610 (1994).
[22] J. H. Underwood, M. K. Gullikson, M. Koike, P. J. Batson, P. E. Denham, K. D. Franck, R. E. Tackaberry, and W. F. Steele, Rev. Sci. Instrum. (to be published).
[23] S. Porowski, I. Grzegory, and J. Jun, in *High Pressure Chemical Synthesis*, edited by B. Baranowski and J. Jurczak (Elsevier, Amsterdam, 1989), p. 21.
[24] J. C. Rife, H. R. Sadeghi, and W. R. Hunter, Rev. Sci. Instrum. **60**, 2064 (1989).
[25] W. R. Hunter and J. C. Rife, Nucl. Instrum. Methods Phys. Res. Sect. A **246**, 465 (1986).
[26] B. W. Veal and A. P. Paulikas, Phys. Rev. B **10**, 1280 (1974).
[27] D. M. Roessler, Br. J. Appl. Phys. **16**, 1359 (1965).